

Renewable hydrogen by autothermal steam reforming of volatile carbohydrates

P.J. Dauenhauer, J.R. Salge, L.D. Schmidt*

Department of Chemical Engineering and Materials Science, University of Minnesota, 421 Washington Ave SE, Minneapolis, MN 55455, USA

Received 26 June 2006; revised 12 September 2006; accepted 12 September 2006

Available online 12 October 2006

Abstract

The autothermal reforming of methanol, ethylene glycol, and glycerol and their solutions in water was examined over platinum- and rhodium-based catalysts supported on alumina foams at a contact time of ~ 10 ms. Catalyst, washcoat, carbon-to-oxygen ratio, and steam-to-carbon ratio were varied to maximize selectivity to H_2 . Rhodium catalysts with the addition of ceria on a γ - Al_2O_3 washcoat layer exhibited the best combination of high fuel conversion and high selectivity to H_2 near equilibrium. Steam addition increased selectivity to H_2 to 89% from methanol, 92% from ethylene glycol, and 79% from glycerol. Selectivity to minor products such as acetaldehyde, ethylene, and methane was $< 2\%$ at optimum conditions for all experiments. The results are interpreted as occurring primarily through surface reactions initiated by adsorption on metals through hydroxyl oxygen lone pairs to form surface alkoxides, which decompose almost exclusively to H_2 and C_1 carbon compounds. © 2006 Elsevier Inc. All rights reserved.

Keywords: Autothermal; Reforming; Carbohydrates; Rhodium; Glycerol

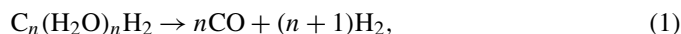
1. Introduction

Biomass provides a significant energy source by converting solar radiation to the biopolymers of plant material through photosynthesis. Frequently considered biomass sources for energy include corn and switchgrass, which consist of a large fraction of carbohydrates. Processes that can convert carbohydrates from these sources to a more usable fuel such as H_2 increase the viability of biomass. Biorefineries currently process the carbohydrate corn starch to ethanol which can be further reformed to H_2 [1]. Conversion to H_2 provides a common energy carrier, allowing other renewable energy sources, such as wind and photovoltaics, to supply power alongside biomass. Direct production of H_2 from carbohydrates catalytically has been demonstrated, but the process requires long reaction times and has shown only $\sim 50\%$ selectivity to H_2 from glucose [2]. Faster reforming of carbohydrates could potentially permit small-scale, low-cost, and distributed H_2 production.

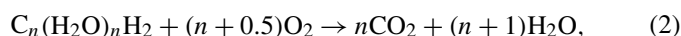
This paper examines the autothermal reforming of methanol, ethylene glycol, and glycerol on noble metal catalysts. These

three molecules represent the first three carbohydrates of formula $C_n(H_2O)_nH_2$ that are both volatile and structurally similar to larger molecules produced in nature, such as glucose. Glycerol is also a side product in the production of biodiesel from triglycerides, and ethylene glycol and glycerol can be produced by the hydrogenolysis of sorbitol [3]. This set of molecules is highly oxygenated with a hydroxyl group on each carbon atom and an internal carbon-to-oxygen ratio (C/O) equal to 1. This presents a challenge for gas-phase reforming with unique chemistry and a significant thermodynamic limitation for synthesis gas production relative to the reforming of alkanes.

Due to high oxygen content, carbohydrate conversion to synthesis gas can occur only stoichiometrically through a decomposition reaction. The decomposition is highly endothermic for methanol ($n = 1$), ethylene glycol ($n = 2$), and glycerol ($n = 3$),



with $\Delta H^\circ = 90, 173, \text{ and } 245$ kJ/mol for $n = 1, 2, \text{ and } 3$. Therefore, autothermal reforming requires thermal energy by producing some complete oxidation products in the highly exothermic combustion reaction,



* Corresponding author. Fax: +1 612 626 7246.
E-mail address: schmi001@cems.umn.edu (L.D. Schmidt).

with $\Delta H^\circ = -676$, -1118 , and -1570 kJ/mol for $n = 1$, 2, and 3. Oxidation at a stoichiometry between Eqs. (1) and (2) permits the catalytic partial oxidation (CPOx) of highly oxygenated molecules for which the conventional equation has been defined by Cubeiro et al. [4],



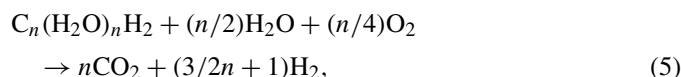
as an exothermic reaction with $\Delta H^\circ = -193$, -393 , and -603 kJ/mol for $n = 1$, 2, and 3. This reaction provides sufficient heat internally to maintain a temperature of 600–1200 °C capable of achieving equilibrium product concentrations at millisecond residence times. Methanol CPOx has been carried out by Traxel et al. on both Pt and Rh catalysts on α -alumina monoliths with typical H_2 selectivity of 65–75% with conversions >90% at low reactant C/O ratios [5]. Further improvements in H_2 selectivity require steam addition to the reactant mixture.

Traditional steam reforming reacts fuel and steam in a highly endothermic process,



with $\Delta H^\circ = 49$, 91, and 123 kJ/mol for $n = 1$, 2, and 3. Steam reforming has been examined at low temperatures in the aqueous phase by Dumesic et al. with selectivity to H_2 as high as 76% from glycerol and 96% from ethylene glycol over tin-promoted Raney-nickel catalysts [6]. Hirai et al. reported that gas-phase steam reforming of glycerol on Ru/Y₂O₃ catalysts exhibited H_2 selectivity of ~90% with a steam-to-carbon ratio (S/C) 3.3 and complete conversion at 600 °C [7].

Fuel conversion can occur faster and without an external heat source applied to the catalyst in a process called autothermal steam reforming (ATSR) in which oxygen, steam, and fuel are all reactants,



with $\Delta H^\circ = -72$, -160 , and -240 kJ/mol for $n = 1$, 2, and 3. Examination of the ATSR of the three carbohydrates can determine the proper feed ratios of fuel, steam and oxygen in addition to the best catalyst for optimizing H_2 selectivity.

2. Experimental

2.1. Reactor

The autothermal reforming of volatile carbohydrates was examined in an 18-mm-i.d., ca. 55-cm-long quartz tube as described previously [15]. The liquid fuel, methanol (Mallinckrodt, >99%) or ethylene glycol (Fisher Scientific, >99%) with or without water, was introduced at room temperature using an automotive fuel injector. The injector produced sufficiently small droplets that permitted rapid vaporization of the liquid fuel in air and on the reactor walls. The fuel was fed to the injector from a fuel tank that was pressurized at 30 psig with a N₂ blanket regulated from a gas cylinder. The fuel injector, operating at 10 Hz, was controlled using LabVIEW software by varying the duty cycle (the percentage of time that the injector

remains open) between 2% and 10%. Fuel delivery exhibited linear behavior with duty cycle and was accurate to within $\pm 2\%$. Glycerol (Alfa Aesar, >99%) and glycerol/water mixtures were pumped into the reactor by a syringe pump due to their high viscosity. All experiments were carried out at atmospheric pressure.

Air was supplied from a regulated gas cylinder at room temperature using a mass flow controller to an inlet 3 cm below the fuel injector. The mass flow controller was operated using LabVIEW software and was accurate to within $\pm 5\%$. To vaporize the fuel, the upper 25 cm of the quartz tube was wrapped in heating tape controlled with a variac. A ceramic foam was wrapped in a ceramic cloth and inserted directly below the heating tape to ensure sufficient mixing of the fuel-air mixture. A chromel-alumel K-type thermocouple was inserted into the quartz reactor 2 cm below the mixing monolith to measure the preheated mixture temperature. Preheat temperatures were maintained at 90, 230, and 300 ± 10 °C for methanol, ethylene glycol, and glycerol, respectively, to ensure a uniform vapor mixture.

Uncoated foams were placed upstream and downstream of the catalyst-coated foam to reduce axial radiation losses from the operating catalysts. The three monoliths were wrapped in ceramic cloth to eliminate gas bypass and then inserted into the reactor ~5 cm below the preheated thermocouple. The downstream uncoated foam monolith had a hole ~2 mm in diameter bored with the reactor axis. A second K-type thermocouple was inserted through the bottom of the quartz tube and through the bottom uncoated foam to measure the backface catalyst operating temperature. Alumina-silica insulation was placed around the reactor to minimize radial heat loss. Product gases were sampled ~5 cm below the bottom uncoated foam at the reactor outlet using a gas-tight syringe.

2.2. Catalyst preparation

All catalysts were supported on ceramic (92% α -Al₂O₃, 8% SiO₂) foams 17 mm in diameter and 10 mm long, with 80 pores per linear inch (ppi) of average channel diameter ~200 μ m. The foams had a nominal surface area of ~1.0 m²/g and a void fraction of ~80%, and were loaded by wet impregnation as described previously [1].

Rhodium and platinum metals were coated on foams by the incipient wetness technique of metal salts [Rh(NO₃)₃, H₂PtCl₆] and subsequent drying in air. Dried catalysts were calcined at 600 °C for 6 h in a closed furnace. Catalysts consisting of only one metal were $5.0 \pm 0.5\%$ (~0.10 g) of the mass of the foam monolith support. Two metal catalysts, rhodium-lanthanum (RhLa) and rhodium-ceria (RhCe), were coated on foams by dropwise addition of a mixture of aqueous solutions of metal salts [Rh(NO₃)₃, Ce(NO₃)₃·6H₂O, or La(NO₃)₃·6H₂O]. A measured amount of solution resulted in ~2.5 wt% each of Rh and Ce or La. Dried catalysts were heated at 600 °C for 6 h in a closed furnace.

A γ -Al₂O₃ washcoat was applied to some catalyst supports before metal loading to increase surface area and decrease channel size [8]. A 3 wt% slurry of γ -Al₂O₃ in distilled water was

applied dropwise to the foam and allowed to dry. The dried foams were then heated at 600 °C for 6 h in a closed furnace. Washcoats were typically 5% by weight of the foam, producing an average alumina film thickness of $\sim 10 \mu\text{m}$. Rhodium and ceria were then loaded as described previously; this catalyst was referred to as rhodium-ceria-washcoat (RhCeWc).

Experimental runs were at least 10 h on any given catalyst, with some catalysts used for as long as 30 h. Almost all experiments were repeated on several catalysts with no significant difference or deactivation. All catalysts were heated to at least 700 °C multiple times during use.

2.3. Product analysis

Gas samples of steady-state reactor products were collected through a septum at the exit of the reactor. A gas-tight syringe wrapped in heating tape and controlled by a variac maintained an internal syringe wall temperature of $\sim 125 \text{ }^\circ\text{C}$. Product samples collected through the septa were injected into a dual-column gas chromatograph equipped with thermal conductivity and flame ionization detectors. Column response factors and retention times were determined by injecting quantities of known species relative to N_2 . Mass balances on carbon and hydrogen typically closed within $\pm 5\%$.

All product selectivities to any species were calculated on an atomic carbon basis, $S_C(\text{species})$, or an atomic hydrogen basis, $S_H(\text{species})$. Selectivity is defined as the (atoms in the product species)/(atoms in the converted fuel). Fuel does not include water. Therefore, the 2 mol of H_2 contained in 1 mol of methanol represents $S_H(\text{H}_2) = 100\%$ regardless of the amount of water added as a reactant. By this definition, $S_H(\text{H}_2)$ can potentially exceed 100% if all of the H atoms from the fuel and some from the water are converted to H_2 . All atomic selectivities based on the same element (C or H) sum to unity within experimental error.

Equilibrium concentrations were calculated at atmospheric pressure, the experimentally observed backface catalyst temperature, and the reactant feed for each C/O and S/C ratio. The equilibrium selectivity to products is included in all figures as dashed lines when capable of providing insight into the results. Allowed species include N_2 , H_2 , O_2 , CO , H_2O , CO_2 , CH_4 , C_2H_6 , C_2H_4 , C_2H_2 , CH_4O , $\text{C}_2\text{H}_4\text{O}$, $\text{C}_2\text{H}_6\text{O}$, and fuel. All equilibrium calculations were carried out using HSC software [9].

3. Results

All experiments were at a constant molar flow rate of 4.0 standard liters per minute (SLPM). The reactant carbon-to-oxygen ratio (C/O) was defined as the moles of carbon in the fuel flow divided by the moles of atomic oxygen in the air flow. By this definition, complete combustion occurs at C/O = 0.33 for methanol, C/O = 0.40 for ethylene glycol, and C/O = 0.43 for glycerol. Experiments varied C/O at ratios higher than combustion stoichiometry in the oxygen-deficient region to sufficiently examine maximum H_2 selectivity. The reactant steam-to-carbon ratio (S/C) was defined as the moles of water divided

by the moles of atomic carbon in the carbohydrate feed. All data points represent the average of three measurements.

3.1. Effect of catalyst

Fig. 1 depicts the CPOx of ethylene glycol on Rh- and Pt-based catalysts. Rh-based catalysts have shown high selectivity for synthesis gas from oxygenated compounds by autothermal reforming [10,11]. Alternatively, autothermal reforming of oxygenates on Pt catalysts exhibited higher selectivity than Rh for such intermediates as ethylene and methane and lower selectivity for synthesis gas [1]. The two metals Ce and La were considered as Rh additives loaded at 2.5 wt% of the foam mass with 2.5 wt% Rh. The additive Ce provides an interesting comparison by increasing surface oxidations rates [12]. Catalysts containing Ce have exhibited enhanced water-gas-shift activity [13], as well as resistance to coke accumulation [14]. La has been investigated as a second additive for comparison.

Reforming of ethylene glycol exhibited steady operation over all experimental conditions. Transient behavior due to a change in operating conditions occurred for a maximum of 3 min. Upstream flames or oxygen breakthrough was not observed for any catalyst. A constant flow rate of 4.0 SLPM corresponded to a GHSV $\sim 10^5 \text{ h}^{-1}$, equivalent to a contact time of $\tau \sim 10 \text{ ms}$ at 700 °C. Conversion at these conditions was $>99\%$ for all catalysts for C/O < 1.6 . Thereafter, each catalyst exhibited a steady decrease in conversion with RhCe $>$ Pt $>$ RhLa $>$ Rh. All catalysts cooled as the reactor feed became more oxygen-deficient, as expected. The three Rh catalysts (Rh, RhCe, and RhLa) operated at about the same temperature with similar behavior; however, the Pt backface temperature was $\sim 30 \text{ }^\circ\text{C}$ higher for C/O < 1.6 and $\sim 30 \text{ }^\circ\text{C}$ lower for C/O > 1.6 .

H_2 selectivity of the four nonwashcoated catalysts exhibited a maximum similar to that observed for other oxygenated compounds [15]. At C/O $< \sim 1.3$, H_2 selectivity decreased with decreasing equilibrium H_2 selectivity. Above C/O ~ 1.4 , H_2 selectivity decreased as the process cooled and slowed down. The order of maximum H_2 selectivity was RhLa (55%) $>$ RhCe (50%) $>$ Rh (43%) $>$ Pt (38%). The Rh-based catalysts exhibited similar CO selectivity of $\sim 75\%$ at lower C/O ratios at which a maximum H_2 selectivity occurred. Pt produced 10–15% less CO than Rh-based catalysts. The remaining carbon resulted in CO_2 and the intermediates ethylene, methane, and acetaldehyde.

Ethylene selectivity was $<2\%$ for all Rh-based catalysts, but up to 5% for Pt. At a C/O = 1.3, ethylene selectivity for RhCe and RhLa was negligible. Maxima were observed for RhCe (1.4%) and RhLa (1.1%) at C/O = 1.9. Rh exhibited a maximum in ethylene selectivity of 1.6% at C/O = 1.7. Similar behavior was observed in methane selectivity. Methane selectivity with Rh-based catalysts never exceeded 9%, whereas methane selectivity on Pt achieved a maximum of 17% at C/O = 1.6. Acetaldehyde selectivity increased steadily with C/O, achieving a maximum of 15–20% on both Pt and Rh-based catalysts. At the maximum H_2 producing C/O = 1.3, the minor products of ethylene, methane, and acetaldehyde did not sum to more than 3% on either RhCe or RhLa.

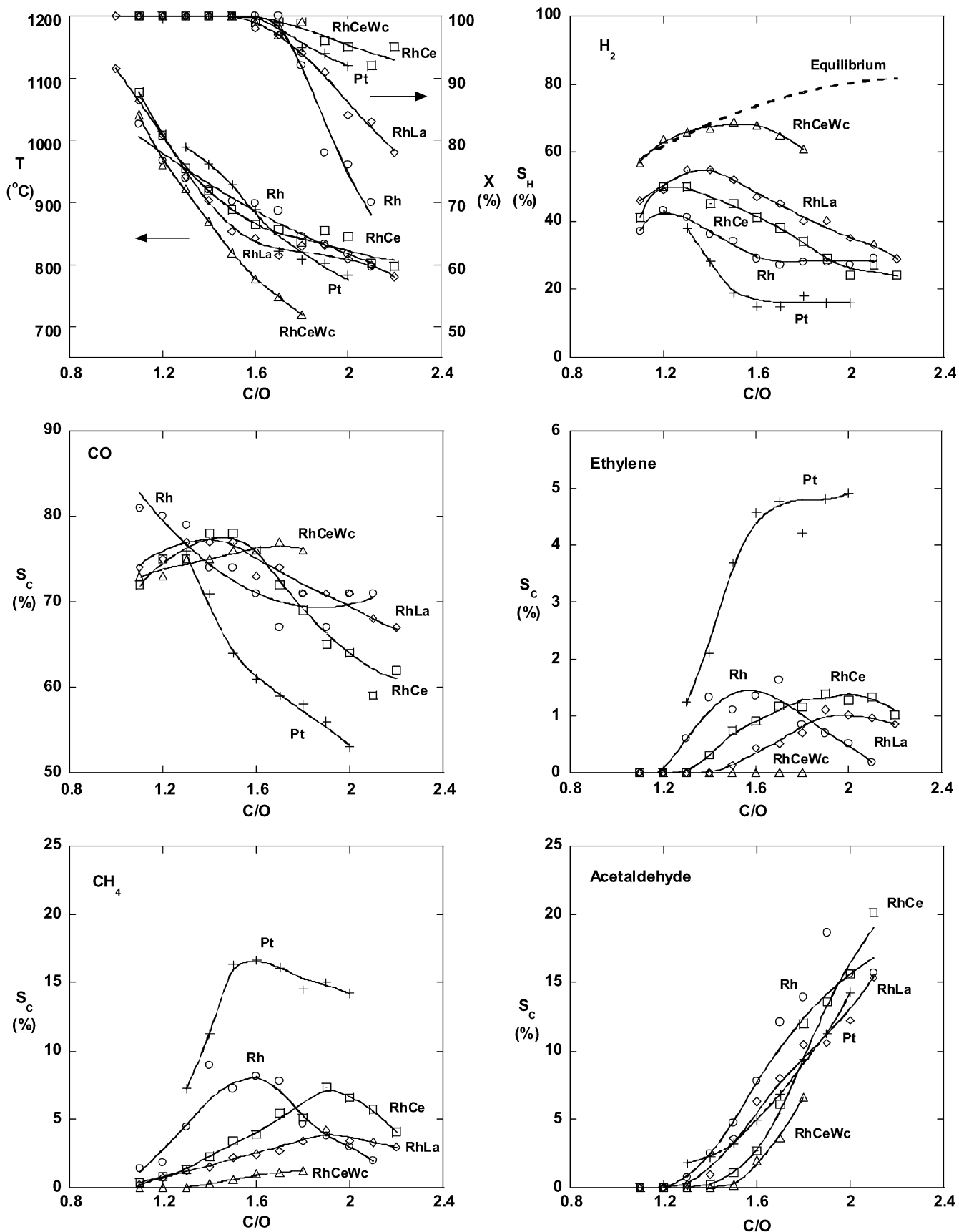


Fig. 1. Catalytic partial oxidation of ethylene glycol on 5 wt% Pt (+), 5 wt% Rh (○), 5 wt% RhCe (□), 5 wt% RhLa (◇), and 5 wt% RhCe on 5 wt% γ -Al₂O₃ washcoat, RhCeWc, (Δ) at 4 SLPM (GHSV ~ 10⁵ h⁻¹). Dashed lines represent equilibrium calculations based on the catalyst back-face operating temperature.

3.2. Effect of washcoat

Fig. 1 includes a comparison of the RhCe and RhCeWc catalyst whereby the sole experimental difference was a 5-wt% γ -alumina washcoat layer applied before catalyst preparation for RhCeWc. The washcoat reduced the backface temperature by $\sim 20^\circ\text{C}$ at low C/O ratios and $\sim 100^\circ\text{C}$ at high C/O ratios. A negligible difference in conversion was observed. Washcoat increased H_2 selectivity from ethylene glycol by approximately 20%. A maximum H_2 selectivity of 69% occurred at $\text{C/O} = 1.5$ with RhCeWc before deviation from equilibrium occurred at $\text{C/O} > 1.6$. In contrast, the washcoat had a nearly negligible effect on CO selectivity.

Washcoat also significantly reduces the production of minor products ethylene, methane, and acetaldehyde. Ethylene was not observed from ethylene glycol with RhCeWc, whereas methane selectivity did not exceed 1%. Acetaldehyde ($\text{C}_2\text{H}_4\text{O}$) was not observed until $\text{C/O} = 1.6$ at which $S_{\text{C}}(\text{C}_2\text{H}_4\text{O}) \sim 2\%$. At the maximum H_2 selectivity C/O ratio of 1.5, the selectivity of minor products do not sum to $> 1\%$. For these reasons, the

RhCeWc catalyst system has been considered for the autothermal reforming of methanol, ethylene glycol, and glycerol with steam addition.

3.3. Autothermal steam reforming of methanol

Fig. 2 shows the temperature, conversion, and measured selectivities of the autothermal reforming of methanol on a 5-wt% RhCeWc catalyst at 4.0 SLPM. Data describing $\text{S/C} = 2$ has been omitted for clarity but has been included in Table 1. The backface temperatures show the dramatic range ~ 400 – 1100°C at which methanol reforms by varying C/O and S/C. The addition of steam to $\text{S/C} = 4.5$ lowers the backface temperature by $\sim 250^\circ\text{C}$ but maintains steady autothermal reforming with negligible effect on conversion. Conversion at both S/C ratios was $> 95\%$ for all C/O ratios.

The relatively low temperatures of the autothermal reforming of methanol at high C/O ratios significantly affects the reaction equilibrium. Significant methanation of the $\text{S/C} = 0$ trial occurs at $\text{C/O} = 1.5$ and above, producing a maximum H_2 equi-

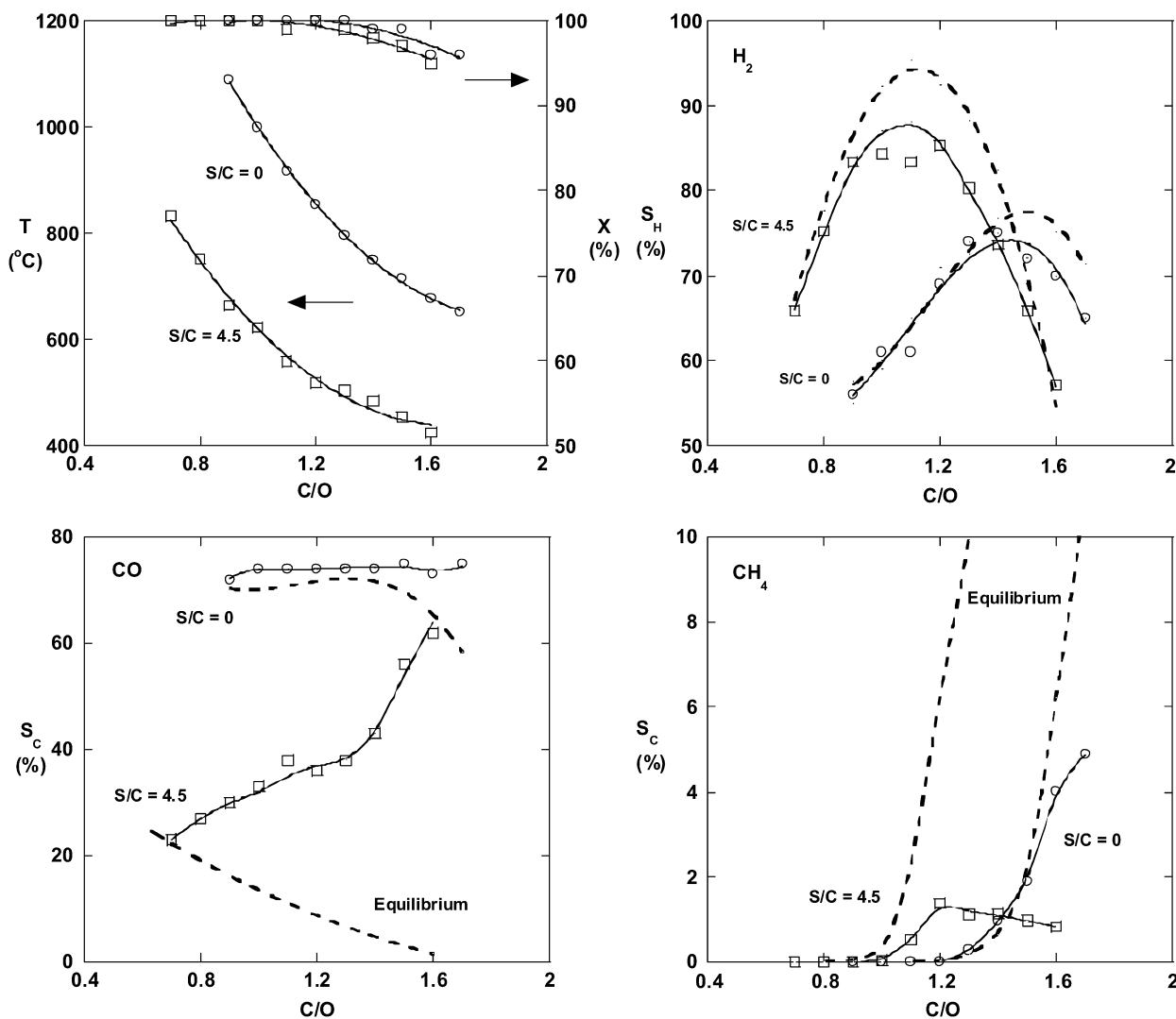


Fig. 2. Autothermal reforming of methanol on 5 wt% RhCe with 5 wt% γ - Al_2O_3 washcoat (RhCeWc) at 4 SLPM ($\text{GHSV} \sim 10^5 \text{ h}^{-1}$) with steam-to-carbon ratios (S/C) of zero (○) and 4.5 (□). Dashed lines represent equilibrium calculations based on the catalyst back-face monolith operating temperature.

Table 1
Selected experimental data for the autothermal reforming of carbohydrates

Catalyst	Methanol			Ethylene glycol				Glycerol		
	RhCeWc	RhCeWc	RhCeWc	Pt	RhCeWc	RhCeWc	RhCeWc	RhCeWc	RhCeWc	RhCeWc
Steam/carbon	0	2	4.5	0	0	2	4.5	0	2	4.5
Carbon/oxygen	1.4	1.2	1.2	1.6	1.5	1.1	1.1	1.2	1.2	0.9
Conversion (%)	99	100	100	100	100	100	100	100	100	100
Temperature (°C)	750	652	519	888	819	802	680	1055	825	862
Hydrogen sel. (%)										
H ₂	75	89	85	15	69	72	92	56	75	79
H ₂ O	24	10	13	54	30	27	8	41	25	21
Carbon sel. (%)										
CO	74	29	36	61	76	62	27	79	58	27
CO ₂	24	70	63	10	23	37	73	19	42	73
CH ₄	1	0.8	1.4	17	0.6	1	0.2	1.1	0.1	–
C ₂ H ₄	–	–	–	5	–	–	–	0.7	–	–
C ₂ H ₄ O	–	–	–	5	0.2	–	–	–	–	0.1
H ₂ /CO	2.0	6.1	4.7	0.4	1.4	1.7	5.1	0.9	1.7	3.9

Note. Experiments were carried out at 4.0 standard liters per minute at atmospheric pressure. RhCeWc catalysts consisted of 2.5 wt% Rh and 2.5 wt% Ce on a 5 wt% γ -Al₂O₃ washcoat supported on 80 ppi α -Al₂O₃ monoliths. Pt catalysts consisted of 5 wt% Pt supported on 80 ppi α -Al₂O₃ monoliths. Selectivity was defined as (C or H atoms in product)/(C or H atoms in converted fuel). Selected RhCeWc data points exhibited a maximum H₂ selectivity.

librium selectivity. This maximum occurs at a lower C/O = 1.1 for the S/C = 4.5 trial, resulting in a severe reduction in the potential for H₂ production thereafter. H₂ selectivity achieves a maximum of 75% for the S/C = 0 trial at C/O = 1.4 and departs from equilibrium at higher C/O ratios. H₂ selectivity of the S/C = 4.5 trial exhibits the behavior predicted by equilibrium producing a maximum of 85% at C/O = 1.2. The remaining hydrogen exited as the products CH₄ and H₂O.

Observed CO selectivity was always greater than that predicted by equilibrium supporting the conclusion that CO is a major intermediate and product. The addition of steam to S/C = 4.5 lowered the CO equilibrium selectivity by ~60%. However, the S/C = 4.5 trial was capable of achieving CO equilibrium only at C/O = 0.7. Similarly, the selectivity for CH₄ in the S/C = 4.5 trial achieved equilibrium only at C/O ~ 0.9 and below. The sum of carbon selectivity (S_C) of all products equaled unity within experimental error with the inclusion of CO₂ (not shown). Thus, the addition of steam resulted in less CO₂ and CH₄ and more CO and H₂O than was predicted by equilibrium.

3.4. Autothermal steam reforming of ethylene glycol

Fig. 3 shows the temperature, conversion, and measured product selectivities of the autothermal reforming of ethylene glycol on a 5-wt% RhCeWc catalyst at 4.0 SLPM. Data describing S/C = 2 was omitted for clarity but has been included in Table 1. The addition of steam at S/C = 4.5 lowers the operating catalyst backface temperature ~250 °C. The reduction in temperature through steam addition had a negligible effect on conversion of ethylene glycol. Conversion >99% was observed for all C/O ratios <1.6 encompassing the operating parameters that maximize H₂ production.

Ethylene glycol reformed at a temperature of ~150 °C greater than that for methanol for almost all C/O ratios, consistent with a preheating temperature difference of 140 ± 10 °C. The slightly higher operating temperature prevented significant

methanation with the S/C = 4.5 trial until C/O = 1.4. The onset of methanation restricted the maximum H₂ equilibrium selectivity to ~110% at C/O = 1.4. The observed process achieved S_H(H₂) = 92% only at C/O = 1.1, with higher C/O ratios resulting in H₂ selectivities significantly less than equilibrium. Thus, the addition of steam to S/C = 4.5 raised the H₂ selectivity by ~30%. The sum of the hydrogen selectivity of all species equaled unity within experimental error with the inclusion of H₂O (not shown).

The observed selectivity to CO in the S/C = 0 trial achieved equilibrium of ~75% for all C/O ratios. The addition of steam to S/C = 4.5 significantly lowered equilibrium selectivity of CO to <20%. However, observed CO selectivity never achieved equilibrium, with a minimum of only S_C(CO) = 27% at C/O = 1.1. Minor products observed in the reactor effluent included methane, acetaldehyde, and trace amounts of ethane and ethylene. Acetaldehyde was not predicted at any significant amount by equilibrium at any C/O and was observed only in trace amounts at the C/O ratio of maximum H₂ selectivity for all S/C. Methane was not observed at S_C(CH₄) > 1% for any C/O despite equilibrium exceeding 10% at C/O > 1.5 for the S/C = 4.5 trial.

3.5. Autothermal steam reforming of glycerol

Fig. 4 shows the temperature, conversion, and measured product selectivities of the autothermal reforming of glycerol on a 5-wt% RhCeWc catalyst at 4.0 SLPM. Data describing S/C = 2 are omitted here for clarity but are included in Table 1. CPOx of glycerol operated with a catalyst backface temperature of ~900–1200 °C for 1.0 < C/O < 1.6. Operating temperatures were approximately ~100 °C higher than those observed with ethylene glycol, consistent with a preheating temperature 70 ± 10 °C warmer. The addition of steam at S/C = 4.5 lowered the backface temperature by ~300 °C. Similar to methanol and ethylene glycol, the change in operating temperature resulted in negligible differences in glycerol conversion. Conversions

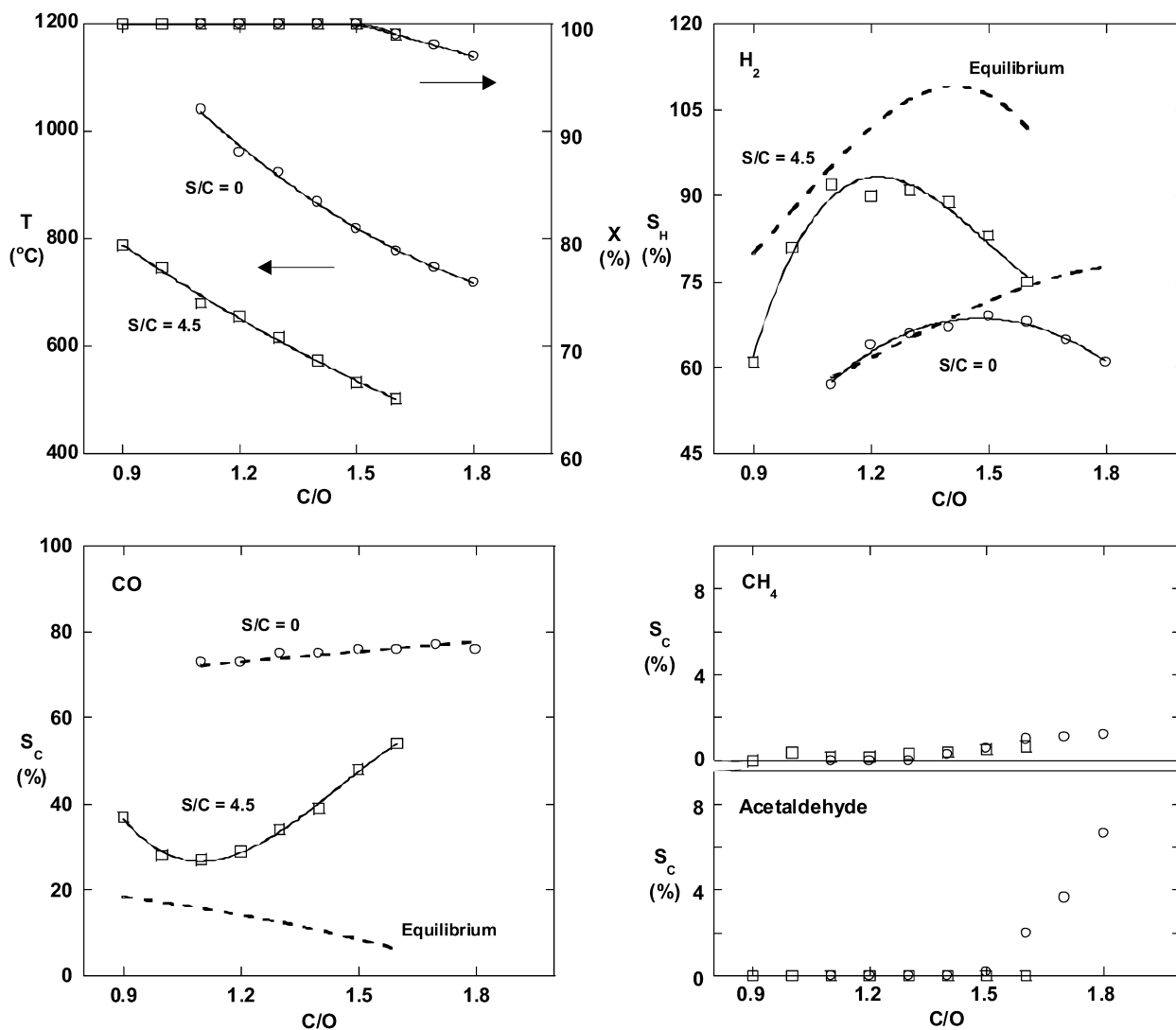


Fig. 3. Autothermal reforming of ethylene glycol on 5 wt% RhCe with 5 wt% γ -Al₂O₃ washcoat (RhCeWc) at 4 SLPM (GHSV $\sim 10^5$ h⁻¹) with steam-to-carbon ratios (S/C) of zero (○) and 4.5 (□). Dashed lines represent equilibrium calculations based on the catalyst back-face monolith operating temperature.

>99% were observed for all C/O and S/C ratios. Steady autothermal reforming was observed at all operating parameters without significant carbon accumulation.

Autothermal reforming of glycerol at S/C = 0 achieved equilibrium H₂ selectivity for all C/O ratios < 1.3 with a maximum of 56% at C/O = 1.2. The addition of steam at S/C = 4.5 increased the equilibrium H₂ selectivity by 30–40%, such that S_H(H₂) = 115% for C/O = 1.6 at equilibrium conditions. However, the observed H₂ selectivity from glycerol departed from equilibrium for C/O > 1.0, producing a maximum of S_H(H₂) = 79% at C/O = 0.9. Data points exceeding equilibrium were within experimental error.

The selectivity to CO was above equilibrium and equal to $\sim 80\%$ for all C/O ratios of the S/C = 0 experiments. The addition of steam lowered the CO equilibrium selectivity by $\sim 50\%$ over the entire C/O range. However, the observed CO selectivity of the S/C = 4.5 experiment departed from equilibrium significantly for C/O > 1.0, producing a minimum S_C(CO) = 25% at C/O = 0.9. The remaining carbon from the reactant fuel was

reformed to CO₂ and the minor products methane, acetaldehyde, ethane, and ethylene. Only trace amounts of ethane and ethylene were observed. Acetaldehyde was not predicted by equilibrium but was observed as high as S_C = 8% at C/O = 1.5 for the S/C = 4.5 experiment. However, at operating parameters producing maxima in H₂ selectivity, S_C < 0.1% of acetaldehyde was observed. Methane was measured at a maximum of S_C(CH₄) = 2% at C/O = 1.6, whereas equilibrium predicted at most S_C(CH₄) = 0.5%.

4. Discussion

The results demonstrate that reforming of carbohydrates by autothermal steam reforming can produce high selectivity to synthesis gas while all minor products exhibit selectivity of no more than S_C $\sim 2\%$ under optimum conditions. Examination of the overall reforming process as well as the surface chemistry of carbohydrates shows that the routes for synthesis gas are favorable, whereas routes for undesirable products are not.

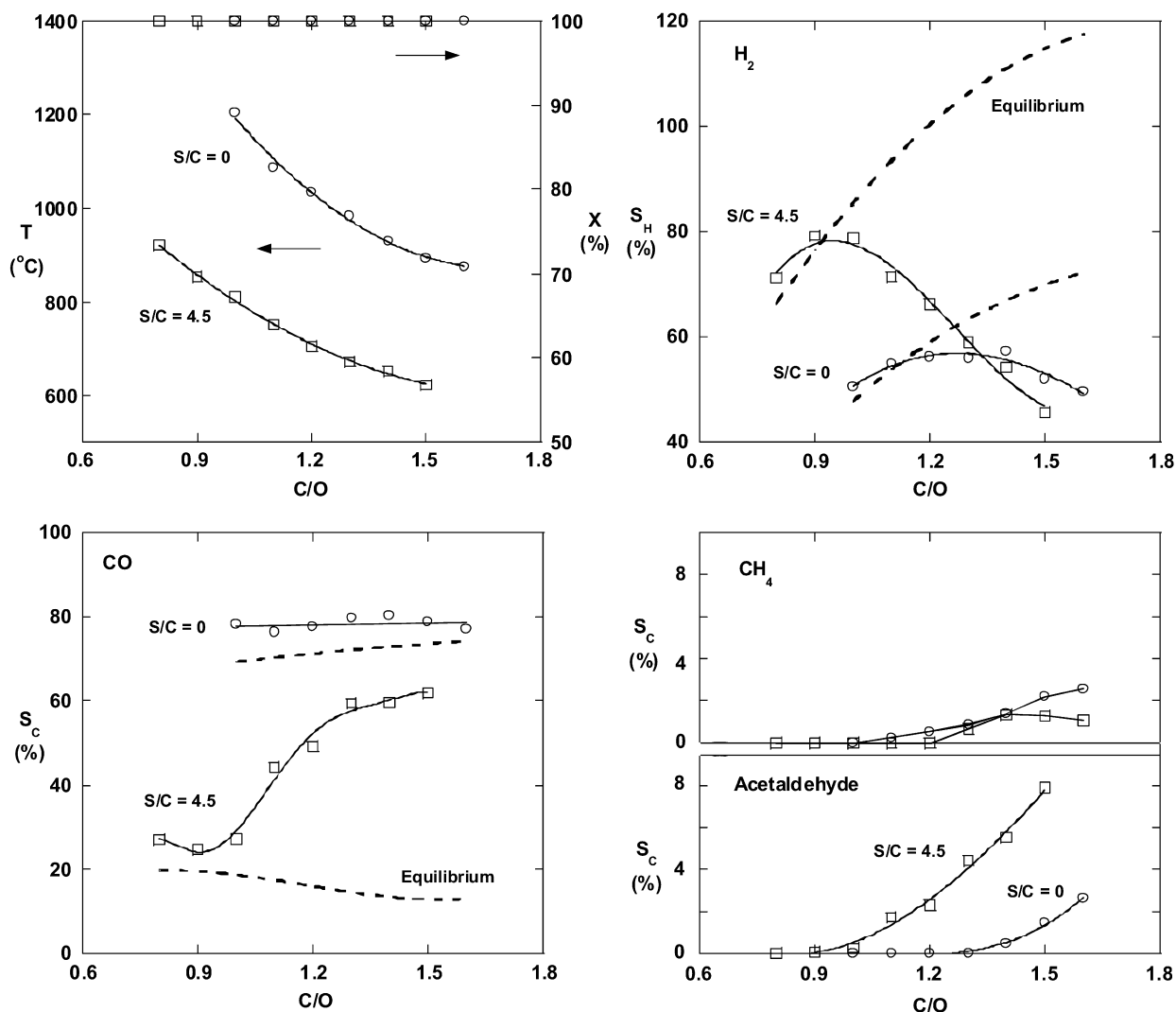


Fig. 4. Autothermal reforming of glycerol on 5 wt% RhCe with 5 wt% γ - Al_2O_3 washcoat (RhCeWc) at 4 SLPM ($\text{GHSV} \sim 10^5 \text{ h}^{-1}$) with steam-to-carbon ratios (S/C) of zero (\circ) and 4.5 (\square). Dashed lines represent equilibrium calculations based on the catalyst back-face monolith operating temperature.

4.1. Millisecond contact time reactor zones

The general model of catalytic partial oxidation of fuels in millisecond contact time reactors involves two distinct reforming zones. Premixed gases entering the catalyst at high velocity and low temperature undergo surface reactions that rapidly raise the operating temperature in <1 ms. Experimental spatial profiles within the catalyst with resolution <1 mm have shown that this oxidation zone exists for the first 1–2 mm, during which $>99\%$ of O_2 is consumed [16]. Surface reactions in this zone likely form much of the thermodynamic products H_2 , H_2O , CO , CO_2 , and CH_4 directly from a large fraction of the reactant fuel and O_2 .

At low C/O ratios, most of the fuel is converted in the oxidation zone. However, as C/O increases, more of the fuel exists past this zone into the remaining 8–9 mm of O_2 -deficient catalyst. Detailed modeling has shown that a fraction of the surface sites in this region of the catalyst are covered by adsorbed carbon [17]. Under these conditions, homogeneous chemistry can become significant, producing nonequilibrium products. En-

dothermic reforming reactions between unreacted fuel and oxidation products lower the gas-phase temperature from the maximum in the oxidation zone. Spatial profiles have shown that the gas-phase temperature observed at the catalyst backface can be 100–150 $^\circ\text{C}$ lower than the maximum temperature [16]. The observed nonequilibrium products are thus affected by both the chemistry specific to the considered fuel and the temperature.

4.2. Mechanisms

Adsorption and decomposition of methanol and ethylene glycol has been studied extensively on noble metal surfaces [18,19]. For example, adsorption of methanol has been examined on both Rh(111) [20] and polycrystalline surfaces [18]. At the high temperature of the oxidation zone (800–1000 $^\circ\text{C}$), the catalytic Rh surface is likely clean with most catalytic sites available [21,22]. Oxygenated compounds containing hydroxyl groups have been shown to adsorb to these open sites predominantly through one or more oxygen atoms. Subsequent decomposition breaking O–H, C–H, C–O, and possibly C–C bonds

produces adsorbed H, C, O, or CO, which then can reform to synthesis gas.

Adsorption of methanol has been shown to occur with one active site through an electron pair on the hydroxyl group [21]. Thereafter, decomposition has been shown in ultra-high vacuum to occur initially through removal of the hydroxyl hydrogen, producing adsorbed methoxide and adsorbed atomic H [20]. Subsequent C–H bond scissions rapidly produce formaldehyde and formyl intermediates and eventually adsorbed CO. Carbon monoxide has been shown to remain essentially nondissociative [18]. A key observation of this mechanism is that once methanol adsorbs, it goes to synthesis gas without the possibility of producing methane or some larger product through dimerization. This agrees with the observed results that CO and H₂ dominate even at high C/O ratios.

Adsorption and decomposition of ethylene glycol occurs similar to that of methanol but with the added complexity of a C–C bond and a second hydroxyl group. Ethylene glycol adsorption on Rh(111) likely occurs through both oxygen atoms [19]. Decomposition occurs initially with O–H scission, producing a dioxy intermediate that will continue to decompose with C–C or C–H scission. The C–O bond was not observed to break, thereby preventing appreciable quantities of products other than CO and H₂ [19]. This is consistent with the high selectivity to synthesis gas products observed experimentally at high C/O ratios. The structure of glycerol is similar to that of ethylene glycol, making it likely that its fastest decomposition route will be similar to that described above.

Acetaldehyde could be produced homogeneously as an intermediate by the dehydration of ethylene glycol and subsequent rearrangement. This intermediate could further adsorb and decompose, making its surface mechanism a possible step. Examination of acetaldehyde on Rh(111) has shown that its adsorption and decomposition are notably different than the carbohydrates [23]. Acetaldehyde adsorbs to two adjacent Rh sites through C and O as $\eta^2(\text{C}, \text{O})$ -acetaldehyde. Scission of the adsorbed carbon C–H bond produces the $\eta^1(\text{C})$ -acyl. This species can break the C–C bond, producing CO and methyl eventually desorbing as methane. This mechanism is consistent with the appearance of methane and acetaldehyde in Fig. 1. Acetaldehyde shows minimal dependence on catalyst, suggesting that it is a homogeneous product. Then at higher C/O ratios, methane selectivity decreases as acetaldehyde increases, making it likely that some of the methane is produced from acetaldehyde decarbonylation.

4.3. Effect of catalyst

Fig. 1 shows that catalyst selection significantly affects selectivity to synthesis gas and the nonequilibrium products ethylene and methane. The addition of Ce or La to Rh raised the synthesis gas selectivity by ~10%. A possible explanation is the ability of Ce to store oxygen, making it available for surface reactions on Rh [12,24]. This could result in faster chemistry, likely increasing the overall rate of partial oxidation. In comparison, Pt produces less H₂ than Rh at higher C/O ratios. Analysis of the adsorption of methanol on polycrystalline Pt surfaces has

shown that decomposition is dominated by the breaking of the C–O bond [18]. C–O bond scission could result in increased levels of adsorbed carbon, fewer available catalytic sites, and an overall slower rate of partial oxidation.

4.4. Effect of washcoat

Addition of a 5-wt% γ -Al₂O₃ washcoat layer to the support before loading the RhCe catalyst was shown to significantly increase selectivity to H₂ and suppress production of nonequilibrium products. Washcoat layers have been found to roughen the support surface, decrease channel size, and increase surface area, thereby increasing mass transfer [8]. Therefore, the lower selectivity to nonequilibrium products from the washcoated catalyst is likely due to the catalyst's ability to transfer these products to the surface and reform them completely to synthesis gas.

4.5. Autothermal steam reforming of carbohydrates

Table 1 summarizes the autothermal reforming of all three carbohydrates at all considered S/C ratios that maximize selectivity to H₂ on RhCeWc catalysts. All three carbohydrates are capable of millisecond reforming, achieving equilibrium at low C/O. Conversion of carbohydrates was high relative to that of less well-oxygenated products under similar operating conditions [1]. In addition, at high C/O, the conversion decreased as the size of the carbohydrate decreased. Mhadeshwar and Vlachos have reported the methanol sticking coefficient on Rh as 0.29, which is ~25% higher than the 0.23 reported for dissociative adsorption of methane on two Rh catalytic sites [21]. The combination of multiple hydroxyl groups adsorbing on multiple Rh sites likely reduces the possibility that an adsorbed carbohydrate could desorb as an unconverted product.

The addition of steam to all three carbohydrates raised the selectivity to H₂ and CO₂ and lowered the selectivity to H₂O and CO. Steam addition at higher S/C ratios raised the equilibrium selectivity to H₂ while lowering the overall operating temperature. Therefore, the maximum selectivity to H₂ occurred at lower C/O as S/C increased in a trend for all three carbohydrates, as shown in Table 1. Reforming occurring at these optimized parameters exhibited only a minor loss of usable energy. For example, conversion of methanol at S/C = 0 and C/O = 1.4 produced an effluent product with ~85% of the availability of the gaseous carbohydrate feed stream. The addition of steam also permitted a tunable synthesis gas ratio (H₂/CO) calculated in Table 1. Maxima in H₂ selectivity exhibited a synthesis gas ratio range $\sim 1 < \text{H}_2/\text{CO} < \sim 5$, including the Fischer–Tropsch optimum of H₂/CO ~ 2 for the production of nonoxygenated fuels [24]. Note again that in Table 1, minor products such as CH₄, ethylene, and acetaldehyde compose a negligible fraction of the reactor effluent at the reactor conditions optimal for maximum H₂ selectivity.

4.6. Catalyst stability

After 10 h of autothermal reforming of ethylene glycol, the α -Al₂O₃ foam supporting 5-wt% Rh without additives weak-

ened significantly and disintegrated, producing a powder. This behavior was not observed on the uncoated α -Al₂O₃ foams placed above and below the Rh catalyst to prevent radiation loss. The Pt, RhCe, and RhLa catalysts also did not exhibit this behavior. Experimental data obtained from the Rh catalyst was collected from multiple samples within the first 8 h.

Disintegration of the Rh/Al₂O₃ catalyst has been observed with the catalytic oxidation of other oxygenated fuels. Salge et al. [1] observed the deterioration of a Rh/Al₂O₃ foam catalyst during the catalytic partial oxidation of ethanol that crumbled to a powder. Similar behavior was also observed by Cavallaro et al. [25] during the steam reforming of ethanol during which Rh crystallites of a powder catalyst appeared to sinter. It was hypothesized that the total oxidation of ethanol at a few locations developed small regions of increased local temperature detrimental to catalyst stability. The specific reason for the disintegration of Rh/Al₂O₃ remains under investigation.

5. Conclusions

The volatile carbohydrates methanol, ethylene glycol, and glycerol were reformed to synthesis gas under autothermal and fast (~10 ms) conditions on noble metal catalysts. High selectivities to H₂ were achieved by adjusting the fuel/air and fuel/steam feed ratios, as well as the catalyst. The addition of steam significantly suppressed CO selectivity while increasing selectivity to H₂ to as high as 92% near equilibrium. Rhodium catalysts with ceria supported on a γ -Al₂O₃ washcoat layer exhibited the best combination of high fuel conversion and H₂ selectivity. Under optimal operating parameters, total selectivity to all minor products was <2%.

For the conditions used in these experiments, surface reactions appear to dominate. Adsorption of all hydroxyl-containing compounds was interpreted as bonding on noble metal surfaces as an alkoxide species that completely decomposes to H₂ and C₁ products. The lack of significant routes to minor products by surface reactions as well as conversion at sufficiently fast rates makes it likely that larger carbohydrates such as glucose, starch, and cellulose can be reformed to synthesis gas.

Acknowledgments

This research was partially supported by grants from the Minnesota Corn Growers Association, the Initiative for Renewable Energy and the Environment at the University of Minnesota, and the U.S. Department of Energy (grant DE-FG02-88ER13878).

References

- [1] J.R. Salge, G.A. Deluga, L.D. Schmidt, *J. Catal.* 235 (2005) 69.
- [2] R.D. Cortright, R.R. Davda, J.A. Dumesic, *Nature* 418 (2002) 964.
- [3] E. Tronconi, N. Ferlazzo, P. Forzatti, I. Pasquon, B. Casale, L. Marini, *Chem. Eng. Sci.* 47 (1992) 2451.
- [4] M.L. Cubeiro, J.L.G. Fierro, *J. Catal.* 179 (1998) 150.
- [5] B.E. Traxel, K.L. Hohn, *Appl. Catal. A* 244 (2003) 129.
- [6] G.W. Huber, J.W. Shabaker, J.A. Dumesic, *Science* 300 (2003) 2075.
- [7] T. Hirai, N. Ikenaga, T. Miyake, T. Suzuki, *Energy Fuels* 19 (2005) 1761.
- [8] A.S. Bodke, S.S. Bharadwaj, L.D. Schmidt, *J. Catal.* 179 (1998) 138.
- [9] Outokumpu Research Oy, HSC Chemistry, version 4.1, <http://www.outokumpu.com/hsc>.
- [10] E.C. Wanat, B. Suman, L.D. Schmidt, *J. Catal.* 235 (2005) 18.
- [11] D.K. Liguras, D.I. Kondarides, X.E. Verykios, *Appl. Catal. B* 43 (2003) 345.
- [12] H. Cordatos, T. Bunluesin, J. Stubenrauch, J.M. Vohs, R.J. Gorte, *J. Phys. Chem.* 100 (1996) 785.
- [13] C. Wheeler, A. Jhalani, E.J. Klein, S. Tummala, L.D. Schmidt, *J. Catal.* 223 (2004) 191.
- [14] T. Zhu, M.F. Flytzani-Stephanopoulos, *Appl. Catal. A* 208 (2001) 403.
- [15] G.A. Deluga, J.R. Salge, L.D. Schmidt, X.E. Verykios, *Science* 303 (2004) 993.
- [16] R. Horn, K.A. Williams, N.J. Degenstein, L.D. Schmidt, *J. Catal.* 242 (2006) 92.
- [17] O. Deutschmann, L.D. Schmidt, *AIChE J.* 44 (1998) 2465.
- [18] M.P. Zum Mallen, L.D. Schmidt, *J. Catal.* 161 (1996) 230.
- [19] N.F. Brown, M.A. Barteau, *J. Phys. Chem.* 98 (1994) 12,737.
- [20] C. Houtman, M.A. Barteau, *Langmuir* 6 (1990) 1558.
- [21] A.B. Mhadeshwar, D.G. Vlachos, *J. Phys. Chem. B* 109 (2005) 16,819.
- [22] C.T. Williams, C.G. Takoudis, M.J. Weaver, *J. Phys. Chem. B* 102 (1998) 406.
- [23] C.J. Houtman, M.A. Barteau, *J. Catal.* 130 (1991) 528.
- [24] M.E. Dry, *Appl. Catal. A* 138 (1996) 319.
- [25] S. Cavallaro, V. Chiodo, A. Vita, S. Freni, *J. Power Sources* 123 (2003) 10.